Polymer Rings and Chains Consisting of Doubly Silyl-Bridged Metallocenes

Frank H. Köhler,* Andreas Schell, and Bernd Weber[a]

Abstract: With the formation of novel organometallic macromolecules in mind, the polycondensation of transition metal ions and bridged cyclopentadienyl ligands was studied. To this end solvated salts MX_2 (M = Fe, Ni, and Cr) were treated with a ligand that consisted of two doubly silyl-bridged cyclopentadienyl anions. For M = Fe and diluted solutions a series of rings $\bigcirc_i$ was obtained that consisted of a minimum of six ($\bigcirc_6$) and up to 17 ($\bigcirc_{17}$) ferrocene moieties in the backbone. They were separated partly by medium pressure liquid chromatography. The macrocycles were established by high-resolution MALDI-TOF mass spectroscopy which also yielded the molecular weight, the polydispersion, and the mean ring size, χ_n, of the mixture of reaction products. When the reaction temperature was decreased from 25 °C to −20 °C, χ_n increased from 8.1 to 10.8. Ferrocene-containing chains, Λ_j, with $2 \le j \le 12$ were obtained in addition to rings in the presence of water; the terminal groups were cyclopentadiene moieties. The reaction of two ferrocene-fused cyclopentadienyl anions with $[FeCl_2(thf)_{1.5}]$ gave chains consisting of exclusively uneven numbers of ferrocenes. For M = Ni and Cr the formation of doubly silyl-bridged nickelocenes and chromocenes was proven by NMR spectroscopy. MALDI-TOF mass spectroscopy showed nickelocene-containing chains accompanied by some rings. For M = Fe the H,H-DQF COSY spectra established the structure of $\bigcirc_7$, $\bigcirc_8$, and $\bigcirc_9$. The oxidation of the ferrocene-containing ring $\bigcirc_7$ with I_2, $NOPF_6$, and $AgPF_6$ gave ionic species $[\bigcirc_7]^{n+}$ which suffered from low stability. The ring-closing reaction is discussed, and the relative abundance of the various rings is related to MNDO calculations.

Keywords: ferrocenes · metallocenes · mass spectroscopy · nickelocenes · polycondensation

Introduction

The use of metallocenes as building blocks is a means to introduce metals into macromolecules. The most popular metallocene in this respect is ferrocene, followed by a wide margin by cobaltocenium ion, while all other metallocenes have been neglected owing to their high reactivity and/or the synthetic effort. Hence, the target compounds are mostly ferrocene-containing dendrimers[1] and polymers[2] which attract attention, because nonlinear optical,[3] semiconducting,[4] liquid crystal,[5] and catalytic[6] behavior as well as applications as sensors[7] and precursors of ceramics[8] have been described. Whenever polymeric materials are being synthesized, the formation of macrocycles besides (branched) chains must be considered, and this topic has been addressed at length.[9] Nevertheless, a rather limited number of rings containing metallocenes (and more generally: sandwich moieties) in the backbone[10] and as pending groups[11] have been well characterized.

We came across the formation of metallocene-containing rings during the investigation of a ligand with two doubly silyl-bridged cyclopentadienyl anions, $\mathbf{1}^{2-}$, (Scheme 1) which aimed at linking metallocenes.[12] Model compounds consisting of two and three metallocenes (Scheme 1, compounds **2** and **3**, respectively) had revealed well-defined electrostatic and magnetic interactions as well as electron spin distributions that depend on the metal and the conformation of the ligand bridge. With the extension of these studies to macromolecules in mind, we looked at the reaction of $\mathbf{1a}^{2-}$ with metal dihalides (Scheme 2) that were expected to yield polycondensation products. The only compound that could be isolated thus far was a macrocycle consisting of seven ferrocenes (Figure 1).[13] This has triggered studies on other macromolecules containing the repeat unit (**1a**M) (M = Fe, Ni) and (**1b**Cr), which are reported here.

Results and Discussion

Restraints upon the formation of rings: It has been established previously that in the dilithium salt, $\mathbf{1a}Li_2$, the bridging ligand is flat owing to Coulomb repulsion of the charges on

[a] Prof. Dr. F. H. Köhler, Dr. A. Schell, Dr. B. Weber
Anorganisch-chemisches Institut
Technische Universität München
85747 Garching (Germany)
Fax: (+49) 89-2891-3762
E-mail: f.h.koehler@lrz.tu-muenchen.de

Supporting information for this article (Figures S1–S10 and calculated dipolar signal shifts of $[\bigcirc_7]^{7+}$) is available on the WWW under http://www.chemeurj.org or from the author.

  0947-6539/02/0822-5219 $ 20.00+.50/0

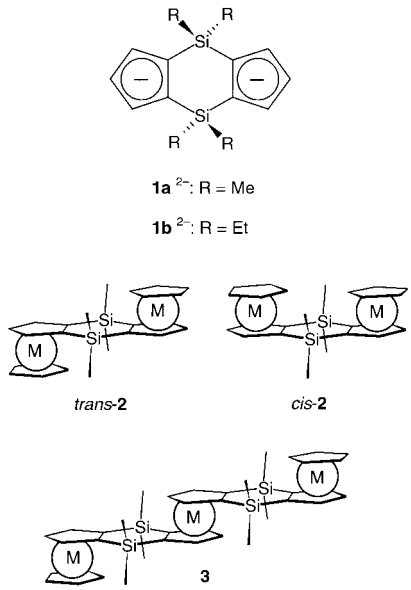

Scheme 1. Di- and trinuclear metallocenes containing the bridging ligands **1a** and **b**.

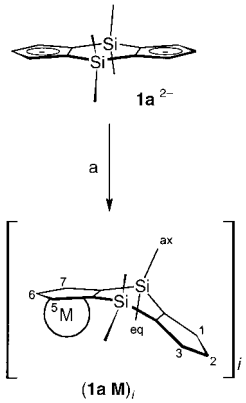

Scheme 2. Synthesis of metallocene rings containing even and uneven numbers of the fragment **1a**M.
a) $[FeCl_2(thf)_{1.5}]$.

the two cyclopentadienyl moieties.[14] Therefore, one would expect that ionic poly(metallocenylene)s derived from the dianion $\mathbf{1a}^{2-}$ prefer to form chains. If the cyclopentadienyl–metal bond is covalent, the bridging ligand should be susceptible to bending about the Si,Si vector and hence to form rings. This has actually been found for di- and trinuclear model compounds[12b,e] and for the ring in Figure 1.[13] The fact that the reaction in Scheme 2 favored a seven-membered ring, $\circ_7$,[15] seemed to indicate that steric hindrance would be a limiting factor of ring formation. But it was unclear whether other rings formed at all, and, if so, how their size would vary. For an estimate MNDO/d calculations[16] on the dinuclear ferrocenes *cis*-**2a**Fe and *trans*-**2a**Fe shown in Scheme 1 and Figure 2 were carried out. The *cis* isomer was included, because this motif has been

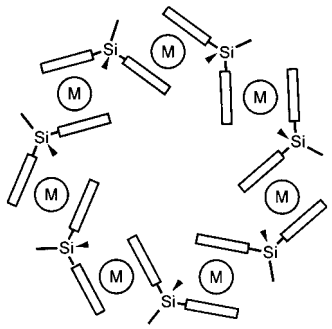

Figure 1. Sketch of a ring consisting of seven ferrocenes (M = Fe).

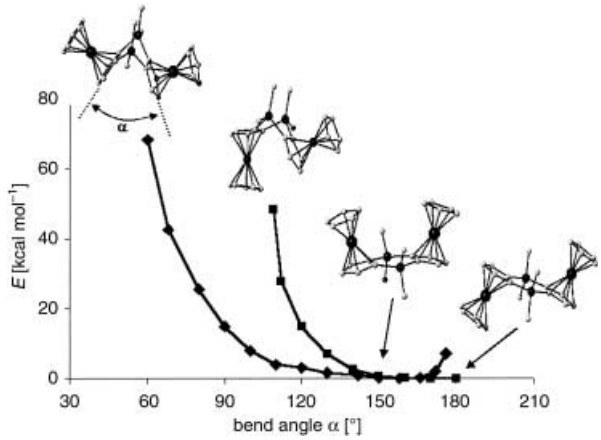

Figure 2. Change of the energies of dinuclear ferrocenes derived from the ligand **1a** with bending; ◆ = *cis* isomer, ■ = *trans* isomer. The energies were scaled to $E = 0$ for $\alpha = 180^\circ$.

established spectroscopically and by crystal structure analysis.[12d,f, 17] Figure 2 shows the change in energy of the *cis* and *trans* isomers with bending. It turns out that the *cis* isomer is more flexible than the *trans* isomer if the angle between the cyclopentadienyl planes does not exceed 180°. Also, for $\circ_7$ with an idealized angle of 128.7° the energy increase is still moderate, while the probability of finding smaller rings decreases drastically.

The formation of rings is also determined by limitations inherent in the polycondensation reaction.[18] Thus, the ring size of a polycondensate decreases with decreasing conversion of the monomer components, unless the conditions of condensative chain polymerization are met.[19] In the present case, a ring consisting of twelve metallocenes would require a conversion of more than 90%.

Synthesis of rings and chains and detection by MALDI-TOF mass spectroscopy: In order to obtain rings larger than $\circ_7$ the polycondensation in Scheme 2 was carried out at 25 °C with the salt **1a**Li_2 and $[FeCl_2(thf)_{1.5}]$ under purified inert gas and carefully controlled stoichiometry (batch A). While this would maximize monomer conversion, highly diluted solutions were used in order to favor ring closure.

Matrix-assisted laser desorption/ionization time of flight mass spectroscopy (MALDI-TOF MS)[20] was applied for the analysis of the product mixtures. The UV/Vis spectrum of the dinuclear model compound *trans*-**2b**Fe[21] (Figure S1, Supporting Information) revealed that the wavelength of the exciting laser hits the absorptions which correspond to those of parent ferrocene.[22] Useful spectra were obtained even without a special matrix, as has been reported in a preliminary paper.[23] It appears that the ferrocene-containing reaction products function as matrix and analyte at the same time. Actually, parent metallocenes are active as cationizing agents prior to desorption in the MALDI process of purely organic polymer standards, as has been found in independent work.[24] In the present case, however, the best spectra were obtained by using known matrices (see Experimental Section). An example is given in Figure 3 which reproduces the spectrum obtained from the product mixture of batch A. The largest peak appears slightly above 2000 Da. It is actually a peak

  0947-6539/02/0822-5220 $ 20.00+.50/0 *Chem. Eur. J.* **2002**, *8*, No. 22

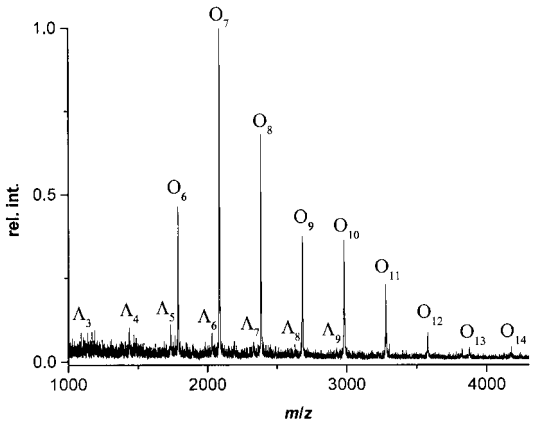

Figure 3. MALDI-TOF mass spectrum of the products obtained from the reaction of **1a**Li_2 with [$FeCl_2(thf)_{1.5}$] at 25 °C under high dilution. $\bigcirc_i$ and Λ_j are rings and chains of the general formula (**1a**Fe)$_i$, and H**1a**(**1a**Fe)$_j$H, respectively.

pattern which perfectly matches the calculated isotope pattern of $\bigcirc_7$ or (**1a**Fe)$_7$ with the most intense mass appearing at 2088.2 Da.[23] On going to higher masses this pattern is followed by other patterns. The difference between adjacent patterns is 298 Da which corresponds to the repeat unit (**1a**Fe), and hence the series establishes macrocycles with up to 14 ferrocenes. Comparison of the calculated and experimental high-resolution patterns confirmed their chemical formula up to $\bigcirc_{11}$; for larger rings the patterns partly disappeared in the noise. Close inspection of Figure 3 reveals a second series of patterns with much lower intensity, which belong to traces of ferrocene-containing chains, Λ_3 through Λ_9[15] (see below).

When the reaction of diluted solutions of **1a**Li_2 and [$FeCl_2(thf)_{1.5}$] was carried out at −20 °C (batch B) the same series of ferrocene-containing rings was observed (Figure S2, Supporting Information), but now the most abundant ring was $\bigcirc_{10}$, while $\bigcirc_7$ and $\bigcirc_{13}$ were about equally present; the series extended to $\bigcirc_{17}$ with a trace of $\bigcirc_{18}$. Analysis of the MALDI-TOF mass spectrum yielded the weight and number averages of the molecular weight, M_w and M_n, respectively, the polydispersity, $P = M_w/M_n$, and the mean ring size, $\chi_n = M_w/m_0$, where m_0 is the molecular weight of the repeat unit. In Table 1 these data are compared with those of other batches.

When equimolar slurries of **1a**Li_2 and [$FeCl_2(thf)_{1.5}$] were used at 25 °C (batch C), two series of peak patterns were found in the MALDI-TOF mass spectrum (Figure S3). The molecular ion of each ring is accompanied by another ion which is 54 Da less, that is, formally each ring loses one iron atom and gains two hydrogen atoms. The general formula of these species is H**1a**(**1a**Fe)$_j$H which represents chains with cyclopentadienes at each end as shown in Figure 4. This is

Table 1. Properties[a] of ferrocene- (M = Fe) and nickelocene-containing (M = Ni) polymers.

Batch[b]	Metal	Product	M_w [Da]	M_n [Da]	P	χ_n
A	Fe	rings	2411	2253	1.1	8.1
B	Fe[c]	rings	3207	3067	1.1	10.8
			3087[e]	1895[e]	1.6[e]	
C	Fe[d]	rings	2529	2426	1.0	8.5
		chains	2093	1756	1.2	7.0
D	Fe	chains	2268	2104	1.6	7.6
	Ni	rings	2101	2073	1.0	7.0
			1076	919	1.2	

[a] From MALDI-TOF mass spectroscopy unless stated otherwise. [b] Diluted solutions, 25 °C, unless stated otherwise. [c] −20 °C. [d] Concentrated solutions. [e] Mixture of rings and chains from GPC.

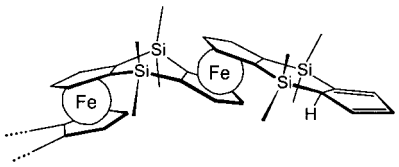

Figure 4. End group of ferrocene-containing chains.

confirmed by the fact that in the mass spectrum the difference between adjacent peak patterns is again 298 Da and that experimental and calculated high-resolution patters are virtually identical. It is worth mentioning that the polymer data of the ring series are similar to those of batch A, that is, dilution is not a deciding factor. In the previous synthesis of $\bigcirc_7$[13] a 100 % excess of [$FeCl_2(thf)_{1.5}$] was used. Repetitions of this procedure yielded reaction mixtures that gave lower M_w and M_n values. This confirms that 1:1 stoichiometry is essential for larger rings and chains.

A second approach to the rings and chains discussed so far is the reaction shown in Scheme 3. The key compound $\mathbf{6}^{2-}$ is a bridged dianion which is expected to react with metal dihalides to give condensation polymers as does the dianion $\mathbf{1a}^{2-}$ in Scheme 2. However, since $\mathbf{6}^{2-}$ contains a ferrocene, the polycondensation is expected to be more selective and produce only rings containing an even number of ferrocenes, that is, compounds **7** in Scheme 3 with the general formula (**1a**Fe)$_{2n}$. A second appealing aspect would be the synthesis of rings that consist of an alternating sequence of two different metallocenes. When the synthesis of the anion $\mathbf{5}^-$[12a] was repeated, it turned out that the mono-deprotonation of the precursor of $\mathbf{5}^-$ is not a clean reaction, and that the dianion $\mathbf{1a}^{2-}$ was formed as well. Therefore, the ferrocene obtained after step a of Scheme 3 was purified by chromatography. Further conversion to the dianion $[\mathbf{6}]^{2-}$ and its reaction with [$FeCl_2(thf)_{1.5}$] (batch D) gave a mixture of products (MALDI-TOF mass spectrum is shown in Figure 5), while the polymer data are given in Table 1. As expected the distance between the peak patterns is now 596 Da, that is, twice the mass of the repeat unit. However, solely chains were detected in repeated experiments. While it is still unclear why rings are missing, the formation of chains that contain only uneven numbers of ferrocenes (compounds **8** in Scheme 3, general formula H**1a**(**1a**Fe)$_{2n+1}$H) confirms the concept of selectively synthesizing metallocene polymers.

All polycondensation reactions described so far started from the bridged cyclopentadienyl dianions $\mathbf{1a}^{2-}$ and $\mathbf{6}^{2-}$. The fact that both are hardly soluble hampers the up-scaling of the reaction, so that some effort is required to meet the stoichiometry. An alternative approach is the reaction of the bridged cyclopentadiene **4** and its isomer[25] with a deprotonating agent that introduces iron at the same time. Tetramesityldiiron,[26] [$Fe_2(mes)_4$], was chosen, because it is well

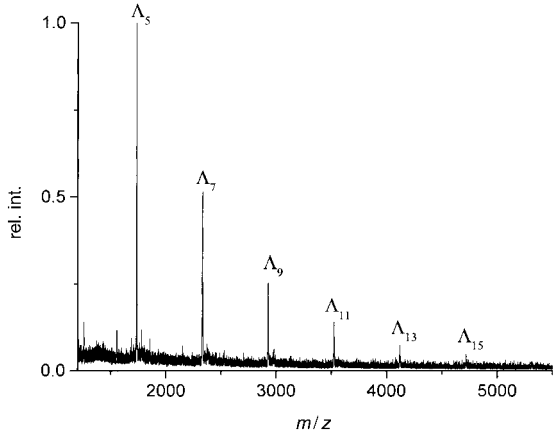

Figure 5. MALDI-TOF mass spectrum of the products obtained from the reaction sequence in Scheme 3. Λ_n are chains of the general formula H**1a**(**1a**Fe)$_{2n+1}$H.

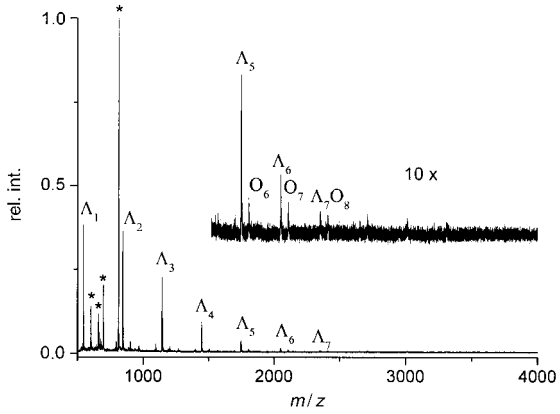

Figure 6. MALDI-TOF mass spectrum of the products obtained from the reaction of **1a**Li$_2$ with [NiCl$_2$(thf)$_{1.5}$] at 25 °C under high dilution. For $\bigcirc_i$ and Λ_j see Figure 3. Impurities are marked by asterisks.

soluble and allows to produce stock solutions where the content can easily be determined by NMR spectroscopy. The reaction of **4** with [Fe$_2$(mes)$_4$] dissolved in THF (Scheme 3, d) did proceed, but only short chains with up to three ferrocenes (compound **8** without brackets) were detected in the MALDI-TOF mass spectra.

The synthesis of rings and chains containing metallocenes other than ferrocene was explored by the reaction of the salts **1a**Li$_2$ with [NiCl$_2$(thf)$_{1.5}$] and **1b**Li$_2$ with [CrCl$_2$(thf)$_{1.6}$]. Although the product mixture had the dark green and red-brown colors typical for nickelocenes and chromocenes, respectively, MALDI-TOF mass spectroscopy was difficult, because the samples were air-sensitive, and their transfer into the spectrometer could not be realized under rigorous exclusion of air. For chromocenes, which are most sensitive, relevant peaks could not be found in the mass spectrum (see, however, NMR results below), while in the case of nickel the result is shown in Figure 6. The series of peak patterns belong to chains that consist of the repeat unit (**1a**Ni) (301 Da) and that are terminated by cyclopentadiene moieties as in the case of the iron analogues. The polymer data in Table 1 indicate that the mean chain length obtained is not favorable for ring formation. Actually, only six-, seven-, and eight-membered rings were detected with low intensity.

Formation of rings and chains: As evident from the MALDI-TOF mass spectra, the isolable ring $\bigcirc_7$ was not only accompanied by larger rings, but also by $\bigcirc_6$. This is in remarkably good agreement with the calculations summarized in Figure 1. From the increase of energy with the bending of the molecule about the Si,Si vector it is clear that, if rings smaller than $\bigcirc_7$ are formed, they should be limited to $\bigcirc_6$. The energy trend visualized in Figure 1 is expected to parallel that of the activation barriers of the ring closure reactions. This explains why $\bigcirc_6$ is always less abundant than $\bigcirc_7$.

More generally, the most important factors which determine the abundance profiles observed in the MALDI-TOF mass spectra are the achievable chain length (which in turn is determined by the monomer conversion) and the strain within the chain just before ring closure. As long as a chain grows, it will be always terminated by iron half-sandwiches of the type CpFeCl(solvent)$_x$.[27] When the chain ends meet, the formation of $\bigcirc_i$ would be preceded by some sort of ring, $\bigcirc'$, consisting of i+1 organometallic moieties. Obviously, $\bigcirc'_{i+1}$ would have a smaller ring strain and hence a lower barrier to formation than $\bigcirc_i$. Conceivable structures of $\bigcirc'_{i+1}$ are halide-fused rings such as the eight-membered species given in Figure 7 (top part). Elimination of FeCl$_2$ and donor solvent molecules from $\bigcirc'_8$ leading to $\bigcirc_7$ is expected to occur readily

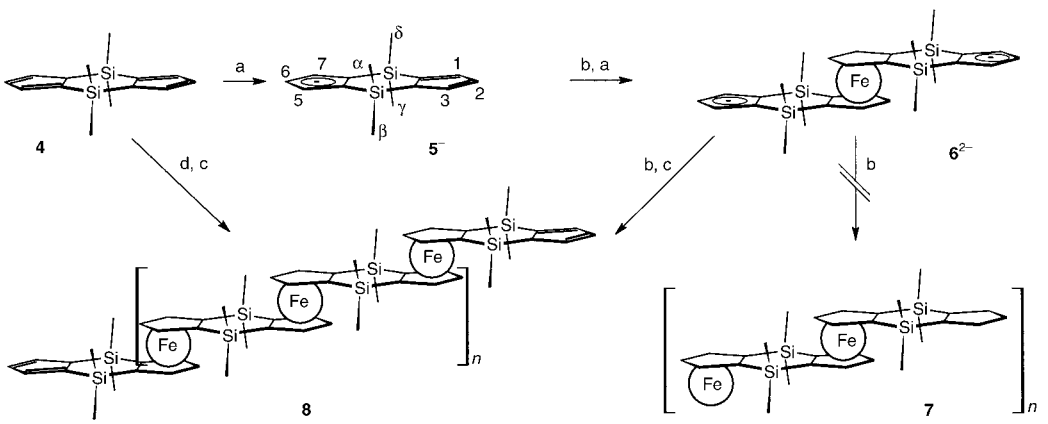

Scheme 3. Synthesis of rings with even numbers and chains with uneven numbers of ferrocenes: a) *n*BuLi; b) [FeCl$_2$(thf)$_{1.5}$]; c) H$_2$O; d) [Fe$_2$(mes)$_4$].

0947-6539/02/0822-5222 $ 20.00+.50/0 *Chem. Eur. J.* **2002**, *8*, No. 22

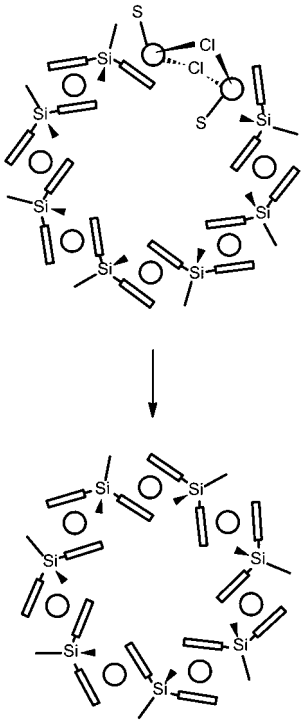

Figure 7. Formation of the ferrocene-containing ring $\circ_7$ by elimination of $FeCl_2$ and solvent (S) from the ring $\circ'_8$.

by analogy to the notorious disproportionation of iron half-sandwiches.[27]

The dependence of the activation barrier on the ring strain also explains the formation of larger rings when the temperature is lowered. For instance, on passing from 25 °C to −20 °C (Figures 3 and S2, respectively) the maximum of the peak profile of the mass spectra was shifted from $\circ_7$ to $\circ_{10}$ and the mean ring size from 8.1 to 10.8 (Table 1). When the polycondensation was carried out at temperatures as low as −78 °C, the mean ring size decreased again. This is ascribed to the decreasing growth rate of the chains. Finally, the fact that the reaction mixture may also contain chains is due to traces of water which transform the terminal iron half-sandwich moieties and/or cyclopentadienyl anions to terminal cyclopentadienes.

Separation and NMR spectroscopy: Gel permeation chromatography (GPC) may be conducted under high-resolution conditions, and this has been applied successfully to organometallic polymers including ferrocene derivatives.[28] When the product mixture obtained from the reaction of the salt **1a**Li_2 with $[FeCl_2(thf)_{1.5}]$ at −20 °C (cf. batch B in Table 1 and Figure S2) was subjected to GPC, an unresolved band was obtained (Figure S4). The molecular weight and the polydispersion were significantly larger than the data resulting from mass spectral analysis. Hence it must be concluded that routinely used polystyrene standards deviate strongly from the shape of the ferrocene-containing rings and chains of this work and that they are of limited utility for calibration.

Oligomeric ferrocenes linked by the bridging ligand **1a** have been separated previously by medium-pressure liquid chromatography (MPLC) up to tetrametallic species including different isomers.[16] However, repeated MPLC runs with samples of batch B gave bands that showed only weak shoulders (Figure S4). Even HPLC experiments using C_{30} phases,[29a] that have been used to facilitate difficult separations including that of isomeric phthalocyanines,[29b] were unsuccessful. Therefore, partial separation of the compounds was attempted by cutting the MPLC band into 20 fractions by collecting the eluents of equal-time intervals. MALDI-TOF mass spectroscopy revealed that the first fraction contained $\circ_7$ and $\circ_8$ in the ratio 7:1 and traces of $\circ_6$, $\circ_9$, and $\circ_{10}$ (Figure S5). The mass spectra of all other fractions did not differ much from that of the initial mixture (Figure S1).

The ^{1}H NMR spectrum of the first MPLC fraction independently proved the formation of $\circ_8$ besides $\circ_7$ in the ratio 7/1, while the traces of $\circ_6$, $\circ_9$, and $\circ_{10}$ could not be detected at the given signal-to-noise ratio. In Figure 8 the set

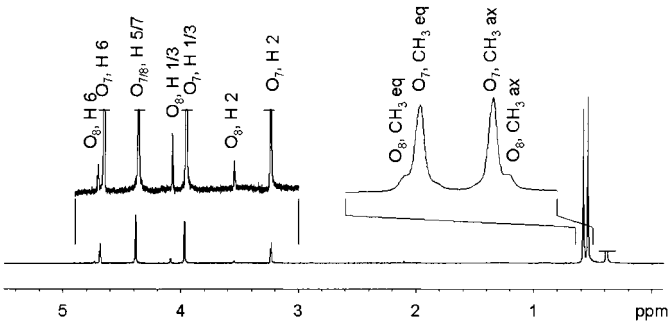

Figure 8. ^{1}H NMR spectrum obtained from the polycondensation products of batch B after MPLC (fraction one of band two). For numbering see Scheme 2.

of small signals has the same features as that of the strong signals which are known from isolated $\circ_7$.[13] The H,H-DQF COSY spectrum (Figure S6) confirms the analogy of the H,H correlations for $\circ_7$ and $\circ_8$ and proves that the signals of H5/7 of both rings coincide at $\delta = 4.37$ ppm. As has been discussed in ref. [13] the unusual signal shift of H2 to low frequency ($\delta = 3.23$ ppm) is due to the fact that H2 projects into the cone of the chemical shift anisotropy of the adjacent ferrocene. This effect must depend on the bending of the bridging ligand, and, actually, for $\circ_8$ the signal of H2 ($\delta = 3.54$) is shifted closer to the usual range of ferrocene protons ($\delta =$ 3.9–4.7 ppm). Both rings $\circ_7$ and $\circ_8$ can also be identified in the H,H-DQF COSY spectrum of the product mixture obtained from batch B (Figure 9), although the resolution is low (as often found for polymers). In addition, $\circ_9$ can be identified by a well-separated cross peak (H2-H1/3), while the correlation between H6 and H5/7 is only partly resolved. It is worth noting that the intensities of the proton signals decrease on passing from $\circ_7$ to $\circ_9$ and that no reliable analysis is possible for bigger rings. The relative abundances of the rings found by ^{1}H NMR spectroscopy and MALDI-TOF MS seems to be different when Figures 9 and S2 are compared. We ascribe this to the formation of an increasing number and amount of isomers with increasing ring size owing to incorporation of *cis*-dimetallic fragments (cf. *cis*-**2** in Scheme 1). These ring isomers would be less symmetric than all-*trans* isomers (e.g. $\circ_7$ in Figure 7) and would give rise to a

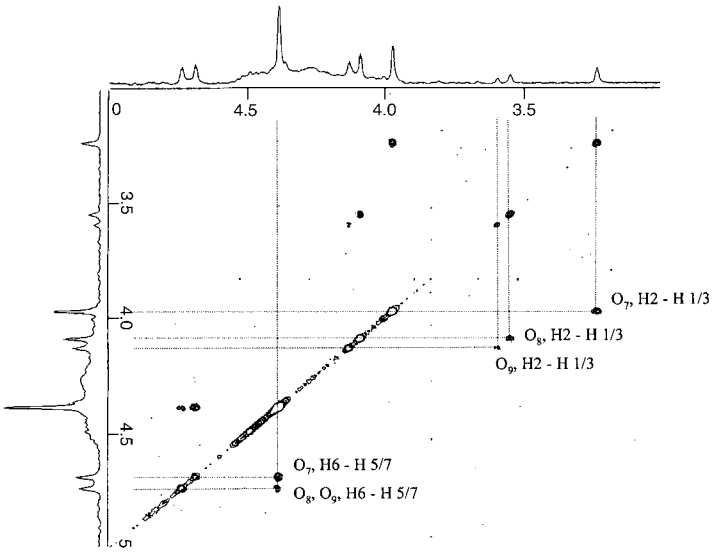

Figure 9. H,H-DQF COSY spectrum of the product mixture obtained from the polycondensation, batch B. The shift range is limited to the proton signals of ferrocenes. The assignment of the cross peaks refers to the respective ring and the protons involved in the correlation. For numbering see Scheme 2.

multitude of signals with low intensities which yield broad features or disappear in the noise.

The product mixtures resulting from the polycondenstion of the dianions $\mathbf{1a}^{2-}$ with $[NiBr_2(thf)_{1.5}]$ and $\mathbf{1b}^{2-}$ with $[CrCl_2(thf)_{1.6}]$ gave ^{1}H NMR spectra that were typical for doubly silyl-bridged nickelocenes and chromocenes, respectively. Thus, in Figure S7 the nickelocene polymers show broad signals for the cyclopentadienyl protons between $\delta = -220$ and -250 ppm; these are signals of silyl groups characteristic for the *trans* arrangement of nickelocene moieties ($\delta = 11-12$ ppm) and for bridges to terminal cyclopentadiene moieties ($\delta = 16-19$ and 0 to -3 ppm). Finally, there are signals of the cyclopentadienes themselves ($\delta = -2$ to -10 ppm). The chemical shift ranges and more detailed signal assignment given in the Experimental Section follow from the comparison with the spectra of the dinuclear nickelocene *trans*-**2a**Ni[12d] and a nickelocene to which two cyclopentadienes are fused.[30] The ^{1}H NMR spectrum of the chromocene polymers (Figure S8) shows signals in ranges that are known from the compound *trans*-**2a**Cr.[12d] Thus, the cyclopentadienyl and $SiCH_2CH_3$ protons appear between $\delta =$ 190 and 260 ppm as well as near -5 ppm, respectively. There are additional signals with paramagnetic shifts up to 15 ppm which are believed to belong to the terminal cyclopentadienes and to $SiCH_2CH_3$. However, no detailed assignment is possible, because a chromocene fused to cyclopentadiene is unknown.

Oxidation of $\circ_7$: From cyclic voltammetry it was known that $\circ_7$ undergoes oxidation in three steps (5, 208, and 403 mV in CH_3CN/CH_2Cl_2 relative to ferrocene), thereby forming tri-, tetra-, and heptacations.[13] Further studies showed that in pure CH_3CN, THF, and 1,2-difluorobenzene the electron transfer beyond the tertracation, $[\circ_7]^{4+}$, becomes irreversible owing to adsorption at the electrode. This led us to monitor the formation of oligo(ferrocenium) ions by ^{1}H NMR spectroscopy during the progressive oxidation of $\circ_7$ in a solution where the polarity was increased continuously. Figure 10 displays a series of spectra starting in the top with pure $\circ_7$ dissolved in C_6D_6. When equal amounts of iodine dissolved in acetone were added, all signals started to shift. As expected from the ^{1}H NMR spectrum of the analogous dinuclear ferrocenium ion *trans*-**2a**Fe^{+}[15] the silyl and cyclopentadienyl proton signals moved to lower and higher frequencies, respectively. For ferrocenium ions the signal half widths of the cyclopentadienyl protons is generally much broader than those of the substituents.[31] Therefore, as the oxidation proceeds, the corresponding signals of $[\circ_7]^{n+}$ seem to disappear in the baseline at the amplification level shown in Figure 10. The signal assignment is derived from that of pure $\circ_7$ except for the silyl protons. The latter can be distinguished, because in the corresponding paramagnetic cations the signals of the equatorial silyl groups are shifted more than those of the axial ones (see Supporting Information). Note that when the oxidation proceeds the silyl signals cross over, and hence the axial and the equatorial silyl signals of $\circ_7$ appear at 0.58 and 0.54 ppm, respectively. The shift trend of the silyl signals in the lower part of Figure 10 indicates that no further

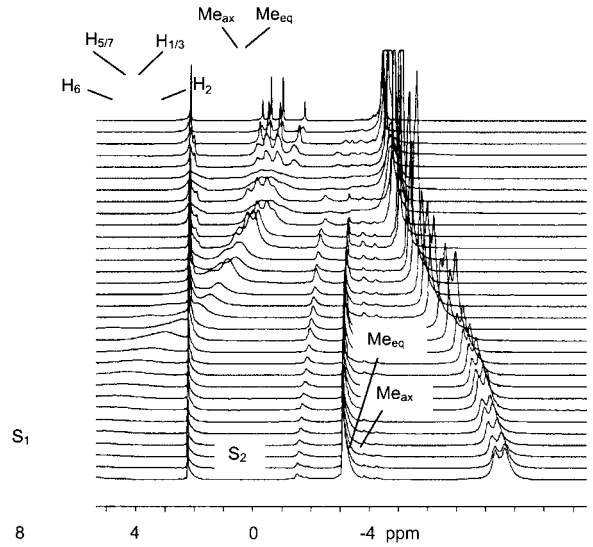

Figure 10. ^{1}H NMR spectra of the oxidation of $\circ_7$ dissolved in C_6D_6 (top trace) by stepwise addition at 305 K of a solution of I_2 in [D_6]acetone. S1 and S2 are the signals of the solvents benzene and acetone, respectively. For numbering see Scheme 2.

oxidation can be achieved, although much larger signal shifts are expected for one positive charge per ferrocene (see below and ref. [17]). The reason is that $\circ_7$ is oxidized only partly by the weak oxidant I_2 and that rapid electron exchange within the ring leads to mean signals for its para- and diamagnetic moieties which have large and small signal shifts, respectiveley.

The more powerful oxidants $NOPF_6$ and $AgNO_3$ in nitromethane gave ^{1}H NMR spectra (Figures S9 and S10) which both show the axial and equatorial silyl signals at $\delta = -20.5$ and -24.3 ppm, respectively. The temperature dependence of these shifts between 253 K and 333 K closely followed the Curie law. The very broad signals of the cyclopentadienyl protons could not be observed, because the solubility of the

  0947-6539/02/0822-5224 $ 20.00+.50/0 *Chem. Eur. J.* **2002**, *8*, No. 22

compound was too low. If the silyl signals belong to $[\circ_7]^{7+}$, the limiting signal shift found for the oxidation with I_2 corresponds to an average of 1.2 charges per $\circ_7$. The spectra recorded immediately after oxidation with $NOPF_6$ and $AgNO_3$ showed additional signals of paramagnetic side products, and we were unable to isolate any well-defined cation. The oxidation with I_2 was also accompanied by decomposition as can be seen in Figure 10 from the signals emerging besides that of acetone. The instability of charged rings might be due to the Coulomb repulsion between positive charges which decreases when the bridging ligand becomes flatter, that is, when the ring breaks. Therefore, one would expect that the stability of the rings $[\circ_i]^{n+}$ decreases with decreasing size and increasing charge.

Conclusion

Polycondensation of the doubly silyl-bridged cyclopentadienyl dianion **1a**$^{2-}$ with $[FeCl_2(thf)_{1.5}]$ and $[NiBr_2(thf)_{1.5}]$ under various conditions does not only yield the previously described seven-membered ring, $\circ_7$, but also other metallocene-containing rings and chains. The latter are terminated by cyclopentadiene moieties which result from the reaction with water. The size of the rings ranges from $\circ_6$ to $\circ_{17}$, and at $-20\,^{\circ}C$ the most abundant ring is $\circ_{10}$ while at $25\,^{\circ}C$ it is $\circ_7$. The abundance of the various rings depends on the ring tension and on the conversion of the monomers: For rings smaller than $\circ_6$ the tension is too strong, and for detectable amounts of rings bigger than $\circ_{18}$ the required monomer conversion of $>94\,\%$ was not achieved. MNDO calculations on model compounds allow estimating trends of the activation barriers of the ring closure reaction.

The method of choice for investigating mixtures of metallocene-containing rings and chains is MALDI-TOF mass spectroscopy. The high-resolution peak pattern of the monocharged molecular ions establish the chemical formula of the different species. Also, the absence of any fragmentation allows to quantitatively determine the abundance of all components and thus the molecular weight, the polydispersion, and the mean ring size or chain length of the sample. Presently, chromatographic separation of the polymer mixtures is limited to samples containing mainly $\circ_7$ and $\circ_8$. NMR spectroscopy proves the structures of $\circ_7$, $\circ_8$, and $\circ_9$ even in the polymer mixture as long as rings without *cis*-arrangement of adjacent ferrocenes are concerned. It is also applicable when paramagnetic nickelocenes and chromocenes are engaged in the polycondensation reaction. And finally, NMR spectroscopy shows that $\circ_7$ can be oxidized to cations that contain ferrocenium ions. These cations are rather unstable due to Coulomb interactions.

Experimental Section

All syntheses and investigations of organometallic compounds were carried out under purified dinitrogen in dry and oxygen-free solvents by using Schlenk techniques. The following starting compounds were prepared following the literature: **1a**Li_2,[14] **1b**Li_2,[21] $[FeCl_2(thf)_{1.5}]$,[32a] $[NiBr_2(thf)_{1.5}]$,[32b] $[CrCl_2(thf)_{1.6}]$;[32c] the chemical formula given here was derived from elemental analyses, which were carried out by the microanalytical laboratory of the authors' institute. The MPLC equipment consisted of a Masterkron 4 HPP pump with pulsation dampener and Sepakron FPGC glass columns from Kronlab and of a Rainin Dynamax UV 1 detector. The columns (15 mm diameter, variable length) were filled with Merck silica 60 (15–40 μm) by applying the slurry-pack procedure. All bands were eluted with hexane, and the absorbance at 300 nm was used for plotting the chromatograms. The GPC equipment consisted of three columns in series packed with polystyrene gel (5 μm particle size, 100 Å pore diameter) from Polymer Laboratories and a Waters 510 HCLP pump. The absorbance at 510 nm was used for plotting the chromatograms.

Spectroscopic measurements and calculations: The mass spectra were recorded by using a Bruker BIFLEX III LDI TOF/RETOF spectrometer equipped with a N_2 laser. The program package XTOF 3.1 was applied for data analysis and simulation. All high-resolution spectra were recorded in the reflectron mode with 10–19 kV and 20 kV accelerator and reflectron voltages, respectively. For the preparation of target spots solutions of 1,8,9-trihydroxyanthracene (dihtranol, 50 mM in THF) and the polymer sample were placed on the target, and the solvent was evaporated. In the case of nickelocene-containig samples the procedure was carried out in a glove box. When the spectra were run without matrix as well as with 2,5-dihydroxybenzoic acid and anthracene, the minimal laser power was lower than in the case of dithranol, and the signal-to-noise ratio was lower. It has been shown previously that the polymer data obtained from MALDI-TOF mass spectra are in good agreement with the results of other techniques.[33] In the present work the data analysis was performed initially by using both the integrals and heights of the peak patterns. In tests up to $m/z \approx 3600$ no significant difference was found, which means that the variation of the pattern widths was so small that it did not affect the data analysis. Therefore, routine analyses were performed with the pattern heights.

The NMR spectra were recorded with a Jeol Lambda 400 spectrometer. The signal shifts were measured relative to the solvent signal and calculated relative to TMS. The UV/Vis spectrum was obtained from a Perkin–Elmer Lambda 2 spectrometer. The MNDO/d calculations were carried out with a Cray t90 computer of the Leibnitz Rechenzentrum München and a SGI workstation by using the programs MNDO94 and UniChem 4.0, respectively.

Reaction of 1aLi_2 with $[FeCl_2(thf)_{1.5}]$

Batch A: From $[FeCl_2(thf)_{1.5}]$ (23.5 mg, 100 μmol) and **1a**Li_2 (25.6 mg, 100 μmol) were prepared pale yellow and colorless solutions in THF (100 mL), respectively. From each stock solution 10 mL were transferred to a Schlenk tube, and the mixture was stirred at $25\,^{\circ}C$ for 6 h. The resulting light brown solution was used for the preparation of the target spots used for MALDI-TOF MS.

Batch B: From each of the stock solutions 10 mL were cooled to $-20\,^{\circ}C$ and transferred to a cooled Schlenk tube. After stirring for 6 h at $-20\,^{\circ}C$ MALDI-TOF MS samples were prepared as described above. For GPC the mixture was reduced to 5 mL and passed over a short column (1 cm silica gel, ambient pressure). The elution was completed with acetone, the solvents were removed in vacuo, the solid remainder was dissolved in THF (2 mL), and this sample was subjected to GPC. The NMR samples were obtained from separate runs. For the spectrum in Figure 9 the solvent of the reaction mixture was removed and replaced by C_6D_6. For the spectra in Figures 8 and S6, THF was removed from the reaction mixture, the solid remainder was dissolved in isopentane (10 mL) and subjected to MPLC (100 cm column length, 25 bar). After rejecting the first small band the second band was eluted in 20 fractions of equal time intervals. All fractions were investigated by MALDI-TOF MS, while the first fraction was used for NMR studies after substituting isopentane for C_6D_6. For elemental analysis the reaction mixture of another run was freed from the solvent and dried in vacuo. Elemental analysis calcd (%) for $(C_{14}H_{18}FeSi_2)_i$ $((298.3)_i)$ C 56.37, H 6.08; found: C 56.28, H 6.20; ^1H NMR (400 MHz, C_6D_6): $\circ_7$: $\delta = 0.54$ (s, 6H, Me_{ax}), 0.58 (s, 6H, Me_{eq}), 3.23 (t, 1H, H2), 3.96 (d, 2H, H1/3), 4.37 (d, 2H, H5/7), 4.68 (t, 1H, H6).

$\circ_8$: $\delta = 0.53$ (s, 6H, Me_{ax}), 0.59 (s, 6H, Me_{eq}), 3.54 (t, 1H, H2), 4.08 (d, 2H, H1/3), 4.37 (d, 2H, H5/7), 4.74 (t, 1H, H6).

$\circ_9$: $\delta = 0.53$ (s, 6H, Me_{ax}), 0.59 (s, 6H, Me_{eq}), 3.60 (t, 1H, H2), 4.13 (d, 2H, H1/3), 4.37 (d, 2H, H5/7), 4.74 (t, 1H, H6).

Batch C: At room temperature **1a**Li_2 (1.00 g, 3.9 mmol) was suspended in THF (50 mL), $[FeCl_2(thf)_{1.5}]$ (0.92 g, 3.9 mmol) was added, and the mixture

was stirred for 1 h. After removing THF, the remaining solid was extracted twice with 50 mL portions of hexane. A small part of the solution was used for the MALDI-TOF MS studies, while the rest was concentrated to a volume of 5 mL, and this was subjected to MPLC (100 cm column length, 25 bar). The large band following a small one was collected, and the solvent was removed in vacuo to yield $(\mathbf{1a}\mathrm{Fe})_7$ (80 mg, 6.9 %), which was spectroscopically pure (MALDI-TOF MS).

Reaction of 6^{2-} with $[FeCl_2(thf)_{1.5}]$

Batch D: The ferrocene-containing cyclopentadienyl dianion $\mathbf{6}^{2-}$ was prepared as described previously[12a] with the following change: The product mixture obtained from the reaction of $\mathbf{5}^-$ with $[FeCl_2(thf)_{1.5}]$ was subjected to MPLC (50 cm column length, 25 bar). From the first orange band a MALDI-TOF mass spectrum was recorded, which only showed the peak pattern of the neutral ferrocene **6** besides that of the matrix dithranol. After deprotonation of **6** to $\mathbf{6}^{2-}$, the reaction of the latter with $[FeCl_2(thf)_{1.5}]$, work-up, and MALDI-TOF MS studies were carried out as described for batch C.

Reaction of 4 with tetramesityldiiron: In a glove box $[Fe_2(mes)_4]$ (28.4 mg, 97 μmol Fe) and the hydrocarbon **4** (13.1 mg, 54 μmol) were placed in a small Schlenk tube and cooled to −78 °C. Subsequently, THF (50 mL) was added by condensation to the cold sample, and the mixture was allowed to reach ambient temperature while stirring overnight. From the resulting light brown solution the target spots for the MALDI-TOF MS runs were prepared.

Reaction of $\mathbf{1a}Li_2$ with $[NiBr_2(thf)_{1.5}]$: A solution of $\mathbf{1a}Li_2$ (23.3 mg, 9.1 μmol) in THF (50 mL) was cooled to 0 °C and transferred through a cannula to a brown solution of $[NiBr_2(thf)_{1.5}]$ (27.9 mg, 9.1 μmol) in THF (50 mL). The resulting black-green mixture was stirred for 2 h, reduced to a volume of 20 mL, and freshly sublimed anthracene (0.5 g) was added. From this solution target spots for MALDI-TOF MS were prepared. The product mixture of a second run was used for NMR spectroscopy. ^{1}H NMR (400 MHz, C_6D_6): $\delta = -1.5$, 0.0, 17.9, 19.4 (Meβ, Meγ, Meδ, and Meα, respectively, of terminal ligand; numbering see Scheme 3), 4.7, 8.2, 10.5 (H1/2, H3, and H3a, respectively, of terminating cyclopentadiene), −234, −243 (nickelocene).

Reaction of $\mathbf{1b}Li_2$ with $[CrCl_2(thf)_{1.6}]$: The reaction and work-up were carried out as described for the nickel analogue by using solutions of $[CrCl_2(thf)_{1.6}]$ (1.2 g, 5.0 mmol) and $\mathbf{1b}Li_2$ (1.6 g, 5.1 mmol). The resulting black solid was used for NMR spectroscopy. ^{1}H NMR (400 MHz, C_6D_6): $\delta = -3.5$ ($SiCH_2CH_3$), 194, 262 (chromocene).

Oxidation of $\circ_7$: A solution of $\circ_7$ (9 mg, 4.3×10^{-3} mmol) in C_6D_6 (0.6 mL) was prepared in a NMR tube. To this solution were added portions of I_2 (6.6 mg, 2.59 10^{-3} mmol) in [D$_6$]acetone (2 mL) in the following sequence: 12 portions of 0.1 equiv (0.016 mL), 5 portions of 0.2 equiv (0.032 mL), 7 portions of 0.5 equiv (0.08 mL), and 6 portions of 1 equiv (0.16 mL). After each addition the components were mixed by shaking the tube, and after waiting for 3 min the NMR spectrum was recorded.

All other oxidations were also carried out in NMR tubes. First, solutions of $\circ_7$ in CD_3NO_2 were frozen at −78 °C. To these samples were added solutions of $NOPF_6$ and $AgPF_6$ in CD_3NO_2, respectively, and rapidly frozen as well. For optimizing the NMR spectrometer the probe head and the sample were held at −50 °C. Subsequently, the samples were brought to ambient temperature, and the spectra were recorded.

Acknowledgement

The assistance of Dr. G. Raudaschl-Sieber (UV/Vis spectroscopy), W. Hieringer (MNDO calculations), and U. Frenzel (GPC) is gratefully acknowledged. We also thank Prof. K. Albert and T. Glaser for HPLC experiments and the Deutsche Forschungsgemeinschaft for financial support.

[1] Dendrimers containing many metallocenes. Reviews: a) C. M. Casado, I. Cuadrado, M. Morán, B. Alonso, B. García, B. Gonzáles, J. Losada, *Coord. Chem. Rev.* **1999**, *185–186*, 53–80; b) G. R. Newcome, E. He, C. N. Moorefield, *Chem. Rev.* **1999**, *99*, 1689–1746; c) I. Cuadrado, M. Morán, C. M. Casado, B. Alonso, J. Losada, *Coord. Chem. Rev.* **1999**, *193–195*, 395–445; d) D. Astruc, J.-C. Blais, E. Cloutet, L. Djakovitch, S. Rigaut, J. Ruiz, V. Sartor, C. Valerio, *Top. Curr. Chem.* **2000**, *210*, 229–259; more recent examples: e) C. M. Casado, B. Gonzáles, I. Cuadrado, B. Alonso, M. Morán, J. Losada, *Angew. Chem.* **2000**, *112*, 2219–2222; *Angew. Chem. Int. Ed.* **2000**, *39*, 2135–2138; f) S. Nlate, J. Ruiz, V. Sartor, R. Navarro, J.-C. Blais, D. Astruc, *Chem. Eur. J.* **2000**, *6*, 2544–2553; g) J. Alvarez, T. Ren, A. E. Kaifer, *Organometallics* **2001**, *20*, 3543–3549.

[2] Polymers containing many metallocenes. Recent reviews: a) K. E. Gonzalves, X. Chen in *Ferrocenes* (Eds.: A. Togni, T. Hayashi), VCH, Weinheim, **1995**, pp. 497–530; b) I. Manners, *Angew. Chem.* **1996**, *108*, 1712–1731; *Angew. Chem. Int. Ed. Engl.* **1996**, *35*, 1603–1621; c) R. P. Kingsborough, T. M. Swager, *Progr. Inorg. Chem.* **1999**, *48*, 123–231; d) R. D. A. Hudson, *J. Organomet. Chem.* **2001**, *637–639*, 47–69.

[3] a) M. E. Wright, E. G. Toplikar, *Macromolecules* **1992**, *25*, 6050–6054; b) T. Itoh, H. Saito, S. Iwatsuki, *J. Polym. Sci. Polym. Chem.* **1995**, *33*, 1589–1596.

[4] a) M. Rosenblum, H. M. Nugent, K. S. Jang, M. M. Labes, W. Cahalane, P. Klemarczyk, W. M. Reiff, *Macromolecules* **1995**, *28*, 6330–6342; b) R. Rulkens, R. Resendes, A. Verma, I. Manners, K. Murti, E. Fossum, P. Miller, *Macromolecules* **1997**, *30*, 8165–8171.

[5] G. Wilbert, S. Trand, R. Zentel, *Macromol. Chem. Phys.* **1997**, *198*, 3769–3787.

[6] D. Astruc, F. Chardac, *Chem. Rev.* **2001**, *101*, 2991–3023.

[7] C. Kim, E. Park, C. K. Song, B. W. Koo, *Synth. Met.* **2001**, *123*, 493–496.

[8] M. J. McLachlan, M. Ginsburg, N. Coombs, N. P. Rajn, J. E. Greedan, G. A. Ozin, I. Manners, *Science* **2000**, *287*, 1460–1463.

[9] U. W. Suter in *Comprehensive Polymer Science* (Ed.: G. Allen), Pergamon Press, Oxford, **1989**, Chapter 6.

[10] a) U. T. Müller-Westerhoff, *Angew. Chem.* **1986**, *98*, 700–716; *Angew. Chem. Int. Ed. Engl.* **1986**, *25*, 702–717; b) S. Barlow, D. O'Hare, *Organometallics* **1996**, *15*, 3885–3890; c) M. Altmann, J. Friedrich, F, Beer, R. Reuter, V. Enkelmann, U. H. F. Bunz, *J. Am. Chem. Soc.* **1997**, *119*, 1472–1473; d) G. Haberhauer, F. Rominger, R. Gleiter, *Angew. Chem.* **1998**, *110*, 3632–3633; *Angew. Chem. Int. Ed.* **1998**, *37*, 3376–3377; e) M. J. McLachlan, J. Zeng, K. Thieme, A. J. Lough, I. Manners, C. Mordas, R. LeSuer, W. E. Geiger, S. M. Liable-Sands, A. L. Rheingold, *Polyhedron* **2000**, *19*, 275–289; f) T. Mizuka, M. Onishi, K. Miyoshi, *Organometallics* **2000**, *19*, 5005–5009.

[11] a) P. D. Beer, *Adv. Mater.* **1994**, *6*, 607–609; b) S. S. H. Mao, F.-Q. Liu, T. D. Tilley, *J. Am. Chem. Soc.* **1998**, *120*, 1193–1206.

[12] a) M. Fritz, J. Hiermeier, N. Hertkorn, F. H. Köhler, G. Müller, G. Reber, O. Steigelmann, *Chem. Ber.* **1991**, *124*, 1531–1539; b) H. Atzkern, J. Hiermeier, B. Kanellakopulos, F. H. Köhler, G. Müller, O. Steigelmann, *J. Chem. Soc. Chem. Commun.* **1991**, 997–999; c) P. Bergerat, J. Blümel, M. Fritz, J. Hiermeier, P. Hudeczek, O. Kahn, F. H. Köhler, *Angew. Chem.* **1992**, *104*, 1285–1287; *Angew. Chem. Int. Ed. Engl.* **1992**, *31*, 1258–1260; d) H. Atzkern, P. Bergerat, M. Fritz, J. Hiermeier, P. Hudeczek, O. Kahn, B. Kanellakopulos, F. H. Köhler, M. Ruhs, *Chem. Ber.* **1994**, *127*, 277–286; e) H. Atzkern, P. Bergerat, H. Beruda, M. Fritz, J. Hiermeier, P. Hudeczek, O. Kahn, F. H. Köhler, M. Paul, B. Weber, *J. Am. Chem. Soc.* **1995**, *117*, 997–1011; f) M. Herker, F. H. Köhler, M. Schwaiger, B. Weber, *J. Organomet. Chem.* in press.

[13] B. Grossmann, J. Heinze, E. Herdtweck, F. H. Köhler, H. Nöth, H. Schwenk, M. Spiegler, W. Wachter, B. Weber, *Angew. Chem.* **1997**, *109*, 384–386; *Angew. Chem. Int. Ed.* **1997**, *36*, 387–389.

[14] J. Hiermeier, F. H. Köhler, G. Müller, *Organometallics* **1991**, *10*, 1787–1793.

[15] Rings and chains were abbreviated by $\circ_i$ and $\mathcal{A}_j$, respectively. The running figures denote the numbers of ferrocene units per macromolecule.

[16] a) M. J. S. Dewar, W. Thiel, *J. Am. Chem. Soc.* **1977**, *99*, 4899–4907 and M. J. S. Dewar, W. Thiel, *J. Am. Chem. Soc.* **1977**, *99*, 4907–4917; b) I. N. Levine, *Quantum Chemistry*, Prentice Hall, London, **1991**.

[17] H. Atzkern, J. Hiermeier, F. H. Köhler, A. Steck, *J. Organomet. Chem.* **1991**, *408*, 281–296.

[18] H. G. Elias, Makromoleküle, Hüthig&Wepf, Basel, **1991**.

[19] T. Yokezawa, H. Suzuki, *J. Am. Chem. Soc.* **1999**, *121*, 11573–11574.

  0947-6539/02/0822-5226 $ 20.00+.50/0

[20] a) M. Karras, F. Hillenkamp, *Anal. Chem.* **1988**, *60*, 2299–2301; b) K. Tanaka, H. Waki, Y. Ido, S. Akita, Y. Yoshida, T. Yoshida, *Rapid Commun. Mass Spectrom.* **1988**, *2*, 151–153.
[21] F. H. Köhler, A. Schell, B. Weber, *J. Organomet. Chem.* **1999**, *575*, 33–38.
[22] Y. S. Sohn, D. N. Hendrickson, H. B. Gray, *J. Am. Chem. Soc.* **1971**, *93*, 3603–3612.
[23] F. H. Köhler, A. Schell, *Rapid Commun. Mass Spectrom.* **1999**, *13*, 1088–1090.
[24] S. K. Poehlein, S. J. Dormady, D. R. McMillin, F. E. Regnier, *Rapid Commun. Mass Spectrom.* **1999**, *13*, 1349–1353.
[25] V. Nakadaira, H. Sakaba, H. Sakurai, *Chem. Lett.* **1980**, 1071–1074.
[26] a) B. Machelett, *Z. Chem.* **1976**, *16*, 116–117; b) H. Müller, W. Seidel, *J. Organomet. Chem.* **1993**, *445*, 133–136.
[27] J. Okuda, *J. Organomet. Chem.* **2001**, *637–639*, 786–792, and references therein.
[28] a) M. Altmann, V. Enkelmann, F. Beer, U. H. F. Bunz, *Organometallics* **1996**, *15*, 394–399; b) O. Nuyken, V. Burkhardt, C. Hübsch, *Makromol. Chem. Phys.* **1996**, *197*, 3343–3354.
[29] a) M. Dachtler, T. Glaser, K. Köhler, K. Albert, *Anal. Chem.* **2001**, *76*, 667–674, and references therein; b) B. Görlach, M. Dachtler, T. Glaser, K. Albert, M. Hanack, *Chem. Eur. J.* **2001**, *7*, 2459–2465.
[30] M. Fritz, J. Hiermeier, F. H. Köhler, *Z. Naturforsch. B* **1994**, *49*, 763–769.
[31] I. Gattinger, M. A. Herker, W. Hiller, F. H. Köhler, *Inorg. Chem.* **1999**, *38*, 2359–2368.
[32] a) R. J. Kern, *J. Inorg. Nucl. Chem.* **1962**, *24*, 1105–1109; b) N. Hebendanz, Dissertation, TU München, **1988**; c) F. H. Köhler in *Organometallic Syntheses* (Eds.: R. B. King, J. J. Eisch), Elsevier, New York, **1988**, pp. 52–55.
[33] a) G. Kuhn, S. Weidner, U. Just, G. Hohner, *J. Chromatogr. A* **1996**, *732*, 111–117; b) J. Bullock, S. Chowdhury, D. Johnston, *Anal. Chem.* **1996**, *68*, 3258–3264; c) M. W. F. Nielsen, S. Malucha, *Rapid Commun. Mass Spectrom.* **1997**, *11*, 1194–1204; d) N. Sakurada, T. Fukuo, R. Arakawa, K. Ute, K. Hatada, *Rapid Commun. Mass Spectrom.* **1998**, *12*, 1895–1898.

Received: April 9, 2002 [F4008]

  0947-6539/02/0822-5227 $ 20.00+.50/0